



This item was submitted to Loughborough's Institutional Repository (<https://dspace.lboro.ac.uk/>) by the author and is made available under the following Creative Commons Licence conditions.



CC creative commons
COMMONS DEED

Attribution-NonCommercial-NoDerivs 2.5

You are free:

- to copy, distribute, display, and perform the work

Under the following conditions:

BY: **Attribution.** You must attribute the work in the manner specified by the author or licensor.

Noncommercial. You may not use this work for commercial purposes.

No Derivative Works. You may not alter, transform, or build upon this work.

- For any reuse or distribution, you must make clear to others the license terms of this work.
- Any of these conditions can be waived if you get permission from the copyright holder.

Your fair use and other rights are in no way affected by the above.

This is a human-readable summary of the [Legal Code \(the full license\)](#).

[Disclaimer](#) 

For the full text of this licence, please go to:
<http://creativecommons.org/licenses/by-nc-nd/2.5/>

ON LASER VIBROMETRY OF ROTATING TARGETS:
EFFECTS OF TORSIONAL AND IN-PLANE VIBRATION

by

S.J.ROTHBERG, J.R.BAKER and N.A.HALLIWELL

ISVR, University of Southampton.

Highfield,

Southampton SO9 5NH,

ENGLAND.

ABSTRACT

Vibration measurements on rotating surfaces are often referred to in the commercial literature as a major application of laser Doppler vibration transducers. This paper examines such use of these instruments and shows how the presence of a velocity component due to the rotation itself leads to spurious measurement dependence on both torsional vibration and motion perpendicular to the line of incidence of the laser beam. In addition, the scale of this dependence increases with both rotation speed and perpendicular distance between the line of incidence and a parallel line through the centre of rotation. These phenomena are investigated theoretically and excellent agreement is found when compared with experimental data. Two solutions are suggested; the first involves careful alignment of the laser beam whereas the second requires two simultaneous, orthogonal measurements to be made. If neither method is adopted it is entirely conceivable that the intended solid body vibration measurement may be masked at many frequencies of interest.

1. INTRODUCTION

Since the advent of the laser in the early 1960's, optical metrology has continued to provide means of remote and unobtrusive measurement in the most challenging of environments. For vibration measurement, several laser Doppler transducers [1-5] have been proposed for situations where use of an accelerometer is precluded such as hot, light and rotating surfaces. The latter case is of particular interest to the engineer who is concerned with rotating and reciprocating machinery where problems with shaft out-of-balance and solid body displacement of rotating components are of concern.

This paper examines the use of laser vibrometers to measure solid body vibration velocity of rotating components and shows that great care is necessary in the interpretation of results. For non-rotating, oscillating targets the vibrometer output is simply a time-resolved voltage analogue of the vibration velocity component in the direction of the incident laser beam. When the target is rotating, however, the additional presence of a velocity component from this motion leads to the output being further dependent upon torsional vibration and motion perpendicular to the incident laser beam. In practice, it is shown that use of a single laser vibrometer may not be able to provide the vibration velocity vector required.

2. THEORETICAL CONSIDERATIONS

2.1 INSTRUMENT PHYSICS

Figure 1 is a schematic diagram which explains the physics of operation of

a laser vibrometer. Scattering particles Doppler shift the incident laser beam by an amount f_D given by [6]:

$$f_D = \frac{2\mu U}{\lambda} \sin (\theta/2) \quad (1)$$

where μ is the refractive index of air, λ is the laser wavelength and θ is the angle defining the scattering direction. The velocity vector, U , bisects the angle $(\Pi-\theta)$ shown in the figure.

Laser vibrometer measurements are usually taken in direct backscatter. With this geometry ($\theta=\Pi$), the Doppler shift on-axis with the incident laser beam is detected. Backscattered light is heterodyned with a frequency shifted reference beam [6] on a photodetector. Demodulation of the photodetector output then produces a time-resolved voltage analogue of the velocity vector, U . In what follows the vibration velocity in the direction of and perpendicular to the incident laser beam are referred to as the on-axis and in-plane components respectively.

2.2 THEORY OF LASER VIBROMETER MEASUREMENTS ON ROTATING SURFACES

In practice, factors such as mass imbalance will cause a rotating shaft to whirl in a complicated manner and, consequently, a unit vector defining the rotation axis will be a function of time. Further to this, at any cross-section, the locus of the centre of rotation will, in general, describe an ellipse. In order to simplify theoretical considerations, however, attention will be limited to the case of a rigid shaft whose centre of rotation describes a narrow ellipse such that motion along the minor axis is negligible.

With reference to figure 2, consider a shaft of arbitrary cross-section and radius vector $\vec{r}(t)$, rotating at speed $N(t)$ about an internal axis defined by the unit vector \hat{z} . The centre of rotation of the shaft undergoes a periodic vector displacement $\vec{x}(t)$ at a constant angle, θ , to the axis of the incident laser beam which is defined by the unit vector \hat{i} . The measured vibration velocity, U_m , will then be the total component of surface velocity in the direction of incidence of the laser beam, given by:

$$U_m = \hat{i} \cdot \frac{d\vec{a}(t)}{dt} + 2\pi N(t) \hat{i} \cdot (\vec{r}(t) \times \hat{z}) \quad (2)$$

where the second term represents the "error velocity", U_e , introduced by virtue of the target rotation. Thus:

$$U_e = 2\pi N(t) \hat{z} \cdot (\hat{i} \times \vec{r}(t)) \quad (3)$$

Examining the vector product:

$$(\hat{i} \times \vec{r}(t)) = |\hat{i}| |\vec{r}(t)| \sin \beta(t) \hat{t} \quad (4)$$

where \hat{t} is a unit vector perpendicular to \hat{i} and $\vec{r}(t)$ and $\beta(t)$ is their included angle. The dimension $y(t)$ may be written:

$$y(t) = |\vec{r}(t)| \sin \beta(t) \quad (5)$$

which allows simplification of equation (3), thus:

$$U_e = 2\pi N(t) y(t) (\hat{z} \cdot \hat{t}) \quad (6)$$

If it is assumed that the shaft rotates without tilt of the rotational axis i.e. the direction of the unit vector \hat{z} is maintained, then expansion of the scalar product yields:

$$U_e = 2\pi N(t) y(t) \cos \alpha \quad (7)$$

where α is the included angle between the unit vectors \hat{z} and \hat{t} . For simplicity has been assumed that $\alpha=0^\circ$ in which case the overall laser measurement may be written:

$$U_m = \left| \frac{d\vec{a}(t)}{dt} \right| \cos \theta + 2\pi N(t) y(t) \quad (8)$$

where the first term represents the intended solid body vibration velocity measurement and the second term is the "error velocity". Expanding time-dependent terms into d.c. and a.c. components using Fourier series:

$$\left| \frac{d\vec{a}(t)}{dt} \right| \cos \theta = \frac{d}{dt} (a_x(t)) = \sum^P (a_p \cos \theta) p\omega_v \sin (p\omega_v t + \psi_p) \quad (9)$$

$$N(t) = N_0 + n(t) \quad \text{where } n(t) = \sum^m n_m \cos (m\omega_T t + \varphi_m) \quad (10)$$

$$y(t) = y_0 + a_y(t) \quad \text{where } a_y(t) = \sum^P (a_p \sin \theta) \cos (p\omega_v t + \psi_p) \quad (11)$$

where N_0 and y_0 are the appropriate mean values, $a_x(t)$ and $a_y(t)$ are, respectively, the on-axis and in-plane components of vibration displacement with fundamental frequency ω_v , $n(t)$ corresponds to torsional vibration with fundamental frequency, ω_T , and ψ_p and φ_m are phase terms. The "error velocity", U_e , may now be written:

$$U_e = 2\pi (N_0 y_0 + N_0 a_y(t) + y_0 n(t) + n(t) a_y(t)) \quad (12)$$

Analysis of each of these terms, none of which pertain to the intended measurement, will allow prediction of an "error spectrum":

(i) $N_0 y_0$: This is a d.c. term and is of little practical interest provided it is not of sufficient magnitude to limit the working range of the instrument.

(ii) $N_0 a_y(t)$: This term indicates the measurement dependence on in-plane vibration, particularly at high rotation speeds where the intended measurement may be masked at all frequencies of interest. Since the in-plane and on-axis components obviously have energy at the same frequencies, this is a very significant term. Importantly, in the absence of torsional vibrations, the measured vibration component at the fundamental vibration frequency may be written, from equations (8) to (11) as:

$$U_m(\omega_v) = (a_1 \cos \theta) \omega_v \sin(\omega_v t + \psi_p) + (a_1 \sin \theta) 2\pi N_0 \cos(\omega_v t + \psi_p) \quad (13)$$

which, for the case where the fundamental vibration frequency equals the rotation frequency, can be simplified to:

$$U_m(\omega_v) = a_1 \omega_v \sin(\omega_v t + \psi_p + \theta) \quad (14)$$

Thus, the amplitude of this frequency component is the modulus of the solid body vibration velocity but it is not possible to resolve any directional information.

(iii) $y_0 n(t)$: This term shows the dependency on torsional vibration, amplified by the mean "off-axis" distance, y_0 , and will result in the presence of spurious information at the torsional vibration frequency.

(iv) $n(t)a_y(t)$: Finally, this cross-term will introduce frequency information at the sum and difference frequencies of solid body and torsional vibration. The amplitudes of the components at these frequencies will be equal and, from equations (10) and (11), are given by:

$$\left| U_e(m\omega_T \pm p\omega_V) \right| = 2\pi \left| \frac{(n_m a_p \sin \theta)}{2} \right| \quad (15)$$

A measurement was made on a test rig with the geometry of figure 2 with θ set to 90° to represent the worst possible case where the intended measurement was nominally zero across the entire spectrum. The output of the instrument is displayed in figure 3 clearly showing these latter three phenomena. For the sake of clarity in the figure, the solid body and torsional motions were induced at distinct frequencies of $\omega_V=6.8\text{Hz}$ and $\omega_T=31.0\text{Hz}$. It must be noted, however, that in many practical situations, the fundamental vibration and torsional frequencies will coincide at the rotation frequency, causing further ambiguity in interpretation of the measurement spectrum. Thus, a spectral peak at the fundamental rotation frequency or a subsequent harmonic may contain information relating to on-axis, in-plane and torsional vibration.

For the case considered, immunity to this error can be achieved through careful alignment of the laser beam. Firstly, the line of incidence should pass through the centre of rotation such that $y_0=0$, eliminating error terms (i) and (iii). In practice this requires adjustment of the height and angle

of the beam until the time-averaged value of the velocity output falls to zero i.e. the d.c term $N_0 y_0$ equals zero. Secondly, the line of incidence of the laser beam must be parallel with the direction of the vibration vector (i.e. $\theta=0$) such that $a_y(t)=0$. This requires adjustment of the point of incidence of the laser beam around the target perimeter until insensitivity to rotation speed as dictated by (ii) is achieved. A second solution is to take two simultaneous, orthogonal solid body vibration measurements and, if necessary, a torsional vibration measurement [7]. Computing power spectra for each allows formation of simultaneous equations to resolve the required vibration components at an individual frequency (ω) of interest. For example, neglecting torsional vibrations, the spectral amplitudes, L_x and L_y , where the subscripts denote direction, are given by:

$$L_x(\omega) = \frac{(\omega a_x)^2}{2} + \frac{(2\pi N_0 a_y)^2}{2} \quad (16a)$$

$$L_y(\omega) = \frac{(\omega a_y)^2}{2} + \frac{(2\pi N_0 a_x)^2}{2} \quad (16b)$$

where a_x and a_y here represent the appropriate vibration displacement amplitudes at frequency ω . Solving these leads to the true components of velocity, U_x and U_y :

$$|U_x(\omega)| = (\omega a_x) = \left[2 \left[\frac{W^2 L_y(\omega) - L_x(\omega)}{W^4 - 1} \right] \right]^{1/2} \quad (17a)$$

$$|U_y(\omega)| = (\omega a_y) = \left[2 \left[\frac{W^2 L_x(\omega) - L_y(\omega)}{W^4 - 1} \right] \right]^{1/2} \quad (17b)$$

where $W = (2\pi N_0/\omega)$. For the case where the vibration frequency of interest is much greater than the rotation frequency, i.e. $W \ll 1$, the above equations reduce to:

$$|U_x(\omega)| = (2L_x(\omega))^{1/2} \quad (18a)$$

$$|U_y(\omega)| = (2L_y(\omega))^{1/2} \quad (18b)$$

which correspond to the intended measurements. Note that no solution is obtainable when $W=1$ except by recourse to equation (14).

It must be remembered, however, that this analysis assumes the direction of the vibration vector to be constant and a solution for the more general case where the centre of rotation describes a wider elliptical path is the subject of continuing work.

3. EXPERIMENTAL WORK

The results of the experimental verification of the error velocity terms in equation (12) are presented in figures 4-7. The geometry of figure 2 was again used and the effect of the parameters N_0 , y_0 , $a_y(t)$ and $n(t)$ investigated. In each figure the solid line represents theoretical data for comparison with the experimental points plotted.

(i) $N_0 a_y(t)$: Under conditions of zero on-axis (i.e. $\theta = \pi/2$) and torsional vibration, finite off-axis distance and an in-plane vibration displacement of 0.235mm, the variation with rotation speed of the apparent vibration

level at the fundamental frequency was noted. From equation (13) the apparent vibration velocity amplitude at this frequency is given by:

$$|U_e(\omega_v)| = | (a_1 \sin \theta) 2\pi N_0 | \quad (19)$$

The results are shown graphically in figure 4. The close agreement between experimental points and the theoretical curve verifies the linear dependence of the apparent vibration velocity on rotation speed as predicted by equation (19).

(ii) $y_{0n}(t)$: Under conditions of zero solid body vibration and torsional vibration of amplitude 3.39rads/s, the variation with mean off-axis distance of the apparent vibration level at the fundamental torsional frequency was studied. From equation (12), this is predicted as:

$$|U_e(\omega_T)| = | 2\pi n_1 y_0 | \quad (20)$$

Figure 5 shows a comparison of the theoretical curve predicted from equation (20) and the experimental results which show excellent agreement.

(iii) $n(t)a_y(t)$: In the presence of both torsional and in-plane vibrations, equal amplitude frequency components are introduced at the sum and difference frequencies of these motion types. From equation (15), the amplitudes at frequencies $(\omega_T \pm \omega_v)$ are given by:

$$|U_e(\omega_T - \omega_v)| = |U_e(\omega_T + \omega_v)| = | \pi (a_1 \sin \theta) n_1 | \quad (21)$$

Verification of this equation is shown in figures 6(a),(b) and 7(a),(b).

For a constant in-plane vibration of amplitude 0.572mm, the torsional vibration amplitude was varied and its effect on the apparent vibration velocity at the frequencies specified above was monitored as illustrated in figures 6(a) and 6(b). Conversely, for a constant torsional vibration of amplitude 3.90rads/s, the in-plane vibration level was varied and its effect on the appropriate component of apparent vibration velocity is shown in figures 7(a) and 7(b). In all cases experimental data shows good agreement with theory.

(iv) The solution suggested in equations (17a&b) was investigated using a modified version of the geometry in figure 2 incorporating two vibrometers aligned perpendicularly in the x and y directions. The rotating target was mounted to allow adjustment of its orientation relative to the fixed x-y axes and measurements were made at a number of values of the angle θ . The vibration velocity components were then resolved, according to equations (17a&b), at the fundamental (6.8Hz) and first two harmonic frequencies. The results are presented in figures 8-10 where the solid line represents theoretical data derived from a prior knowledge of the true magnitude and direction of the vibration vector and experimental points are plotted for comparison. Excellent agreement is found at the fundamental vibration frequency in both x and y directions as shown in figures 8(a) and 8(b).

Such close agreement is not found, however, in the subsequent figures showing power spectrum levels at the first and second harmonic frequencies, illustrating important limitations of this technique. Figures 9(a) and 9(b) show data at the first harmonic frequency where low vibration levels approaching the noise-floor of the instruments have affected the accuracy with which equations (17a&b) may be implemented. Figures 10(a) and 10(b) show data at the second harmonic frequency where the ratio of the rotation

frequency (17Hz) to the vibration frequency is close to unity and, consequently, the denominator in equations (17a&b) tends to zero, compounding measurement errors.

4. CONCLUSIONS

Vibration measurements on rotating surfaces are often referred to in the commercial literature as a major application of laser Doppler vibration transducers. However, in this paper, it has been demonstrated how the measurement can show spurious dependence on in-plane and torsional vibration, rotation speed and off-axis distance for the case of a solid body vibration vector of constant direction. The effect of each of these parameters on the "error velocity" has been investigated experimentally and found to be in excellent agreement with theoretical predictions.

For the case considered, these problems can be avoided by arranging for the line of incidence of the laser beam to be parallel to the shaft vibration vector while passing through the centre of rotation of the shaft. Alternatively, two concurrent, orthogonal vibration measurements, in conjunction with a torsional vibration measurement if necessary, will allow solution of simultaneous equations at any individual frequency to yield the true vibration velocities. This is not the case, however, at the rotation frequency where it is only possible to evaluate the modulus of the vibration vector. It should also be noted that at frequencies of interest much higher than the rotation frequency the measured spectral amplitudes will approximate to those of the true vibration velocity components.

In the absence of such measures, it is entirely conceivable that the

intended measurement may be masked at many frequencies of interest, particularly when the fundamental solid body and torsional vibration frequencies coincide at the rotation frequency. This will be true in many cases of engineering interest.

REFERENCES

- [1] J.OLDENGARM, A.H.VON KRIEKEN and H.RATERINK 1973 Optics and Laser Technology 5, 249-252 Laser Doppler Velocimeter with Optical Frequency Shifting
- [2] P.BUCHAVE 1975 Optics and Laser Technology 7, 11-16, Laser Doppler Velocimeter with Variable Optical Frequency Shift.
- [3] C.J.D.PICKERING, N.A.HALLIWELL and T.H.WILMSHURST 1986 J.Sound and Vib. 107(3), 471-485, The Laser Vibrometer: A Portable Instrument
- [4] R.I.LAMING, M.P.GOLD, D.M.PAYNE and N.A.HALLIWELL 1986 Electron.Lett. 22, 167-168, Fibre-Optic Vibration Probe.
- [5] J.R.BAKER, T.H.WILMSHURST and N.A.HALLIWELL, "A New High Sensitivity Laser Vibrometer", to be published.
- [6] F.DURST, A.MELLING and J.H.WHITELAW 1981 Principles and Practice of Laser Doppler Anemometry. London: Academic Press, second edition
- [7] N.A.HALLIWELL, C.J.D.PICKERING and P.G.EASTWOOD, "The Laser Torsional Vibrometer: A New Instrument", J.Sound and Vib., 93(4), pp588-592, 1984

FIGURES

Figure 1: Doppler Shift of Laser Beam by Scattering Particles

Figure 2: Geometry of Measurement Set-Up

Figure 3: Instrument Output Showing Spurious Dependence on In-Plane and Torsional Vibration

Figure 4: Effect of Rotation Speed during In-Plane Vibration

Figure 5: Effect of Mean "Off-Axis" Distance during Torsional Vibration

Figure 6: Effect of Torsional Vibration during In-Plane Vibration

(a) Difference Frequency (b) Sum Frequency

Figure 7: Effect of In-Plane Vibration during Torsional Vibration

(a) Difference Frequency (b) Sum Frequency

Figure 8: (a) Resolved X-Axis Component - Fundamental Frequency

(b) Resolved Y-Axis Component - Fundamental Frequency

Figure 9: (a) Resolved X-Axis Component - 2 x Fundamental Frequency

(b) Resolved Y-Axis Component - 2 x Fundamental Frequency

Figure 10: (a) Resolved X-Axis Component - 3 x Fundamental Frequency

(b) Resolved Y-Axis Component - 3 x Fundamental Frequency

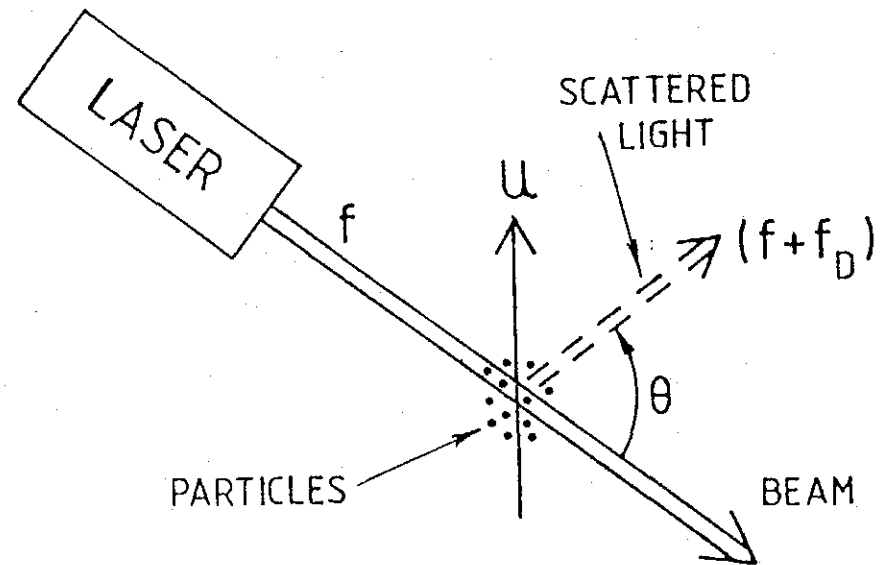


Figure 1: Doppler Shift of Laser Beam by Scattering Particles

W1 AUTO SPEC CH. A [] STORED MAIN Y: -111.6dB
 Y: -27.0dB /1.00U RMS 40dB BPO X: 0.000Hz
 X: 0.000Hz + 50Hz LIN
 SETUP S2 #A: 20

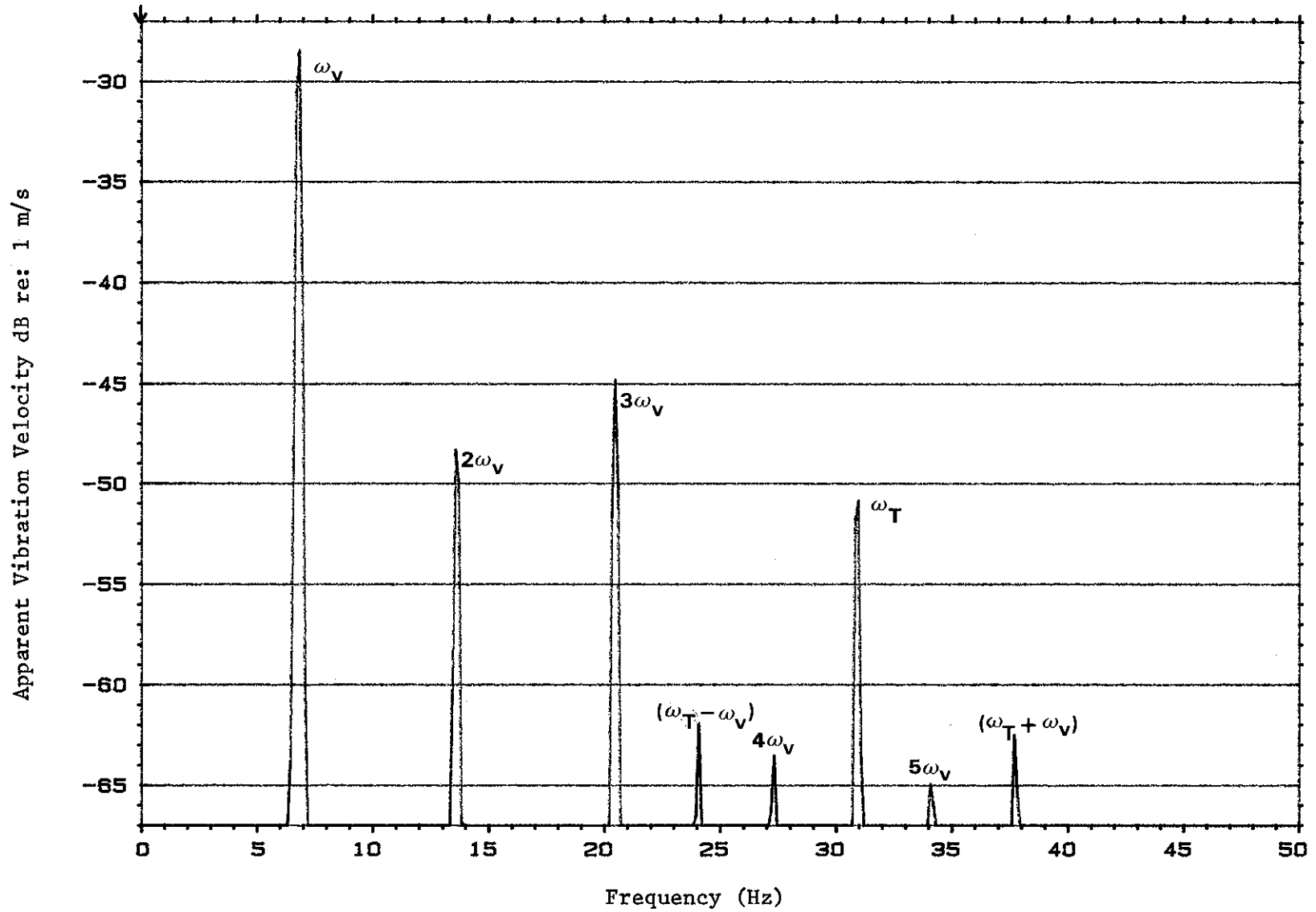
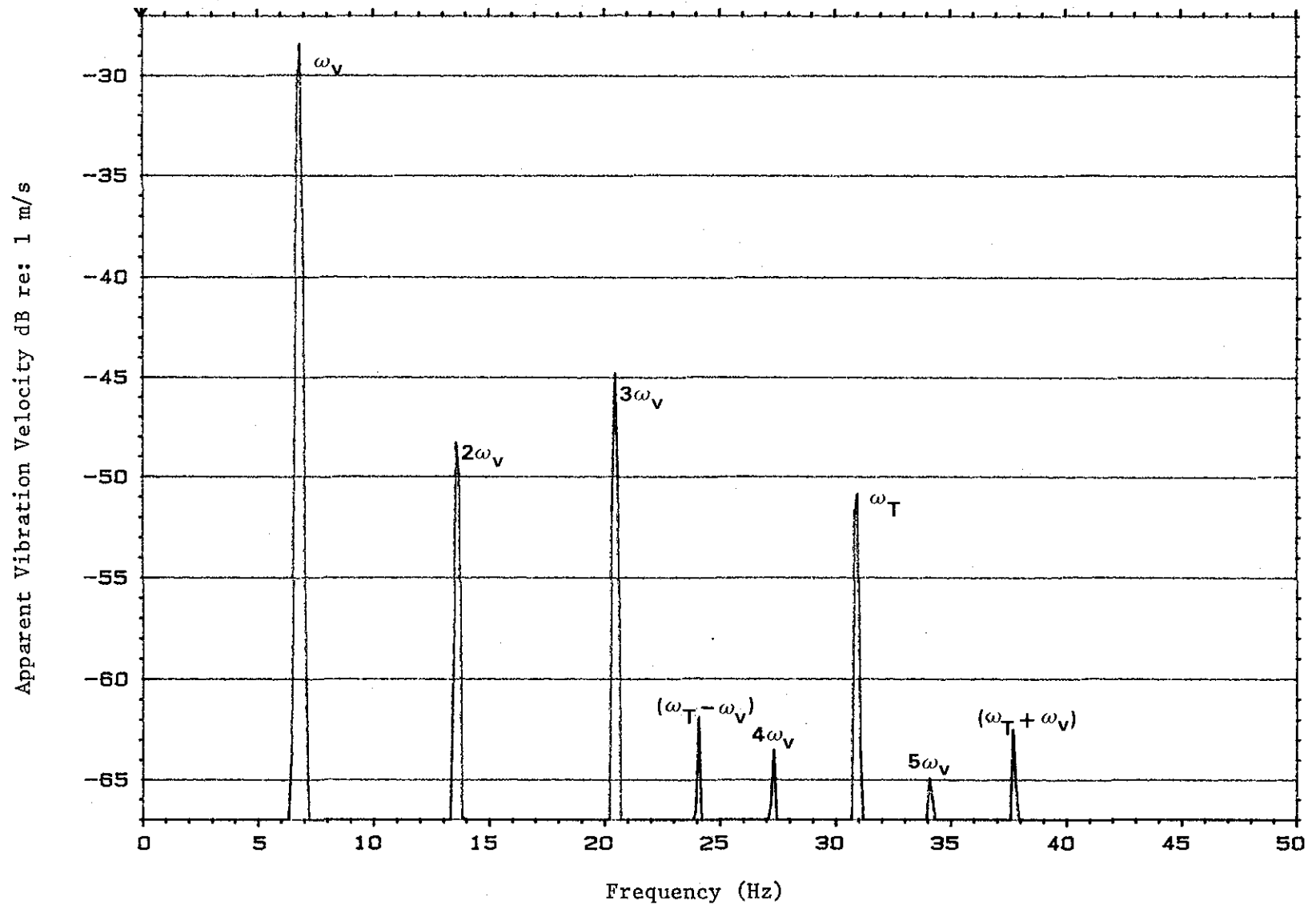


Figure 3: Instrument Output Showing Spurious Dependence on In-Plane and Torsional Vibration



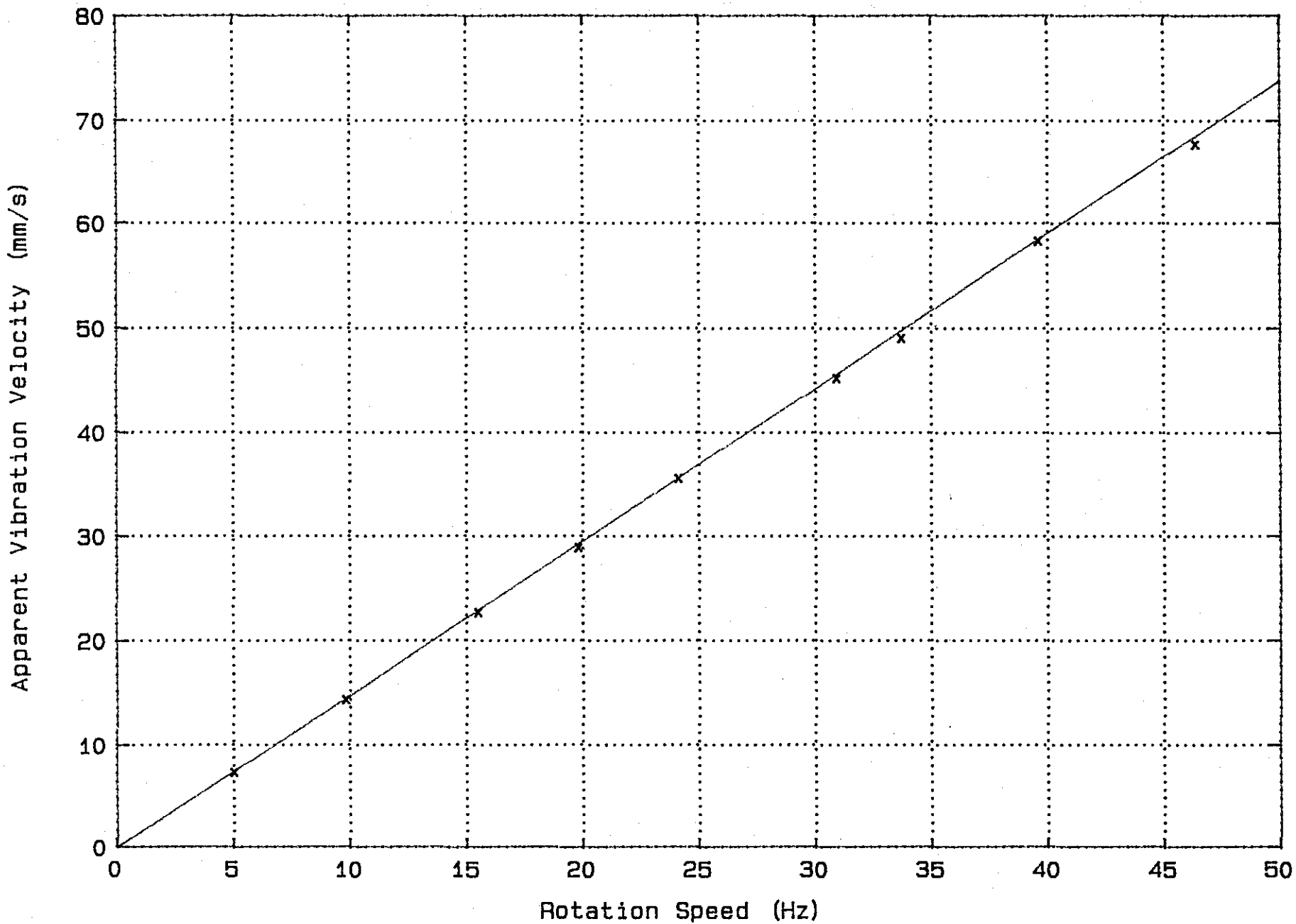


Figure 4: Effect of Rotation Speed during In-Plane Vibration

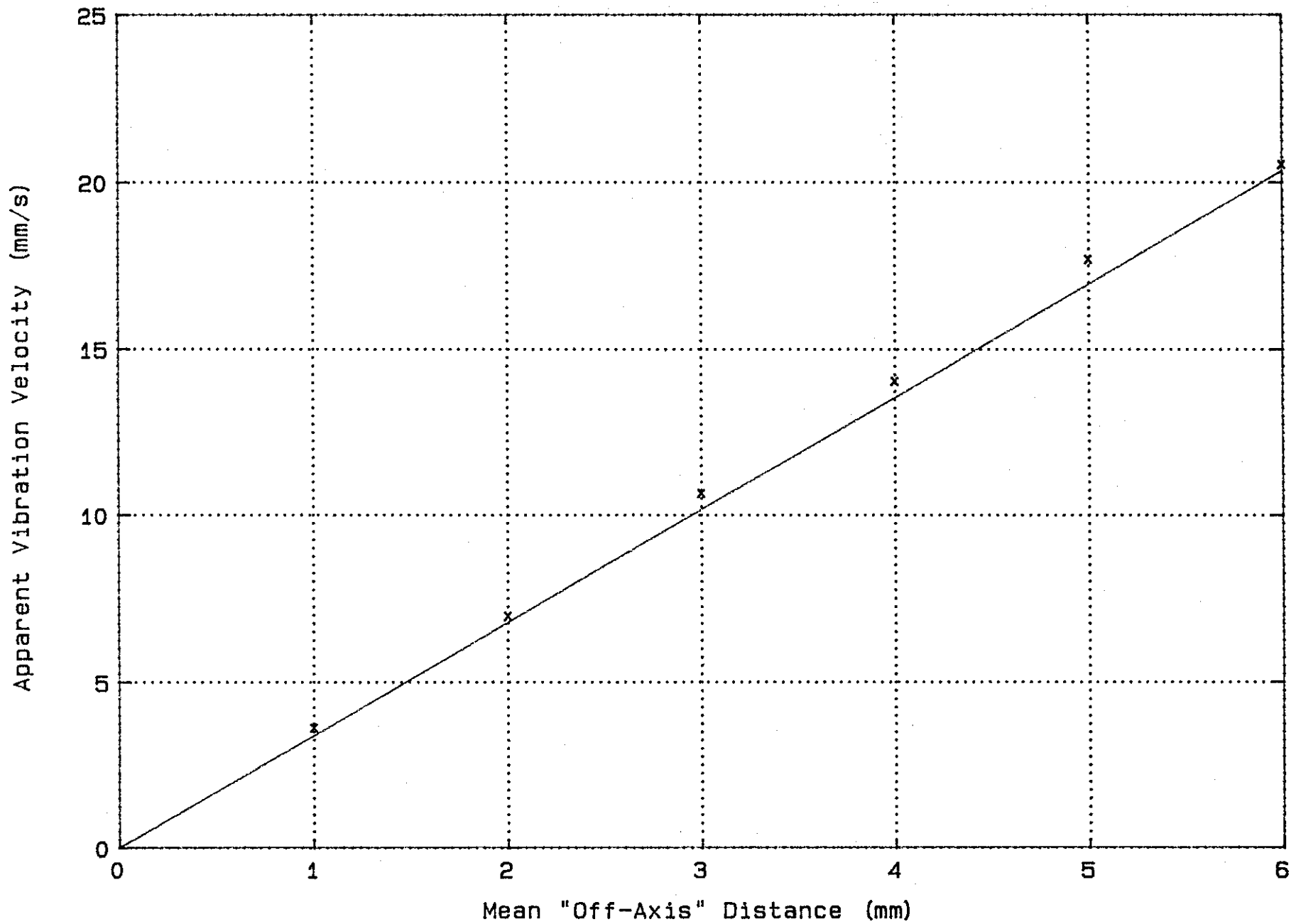


Figure 5: Effect of Mean 'Off-Axis' Distance during Torsional Vibration

555

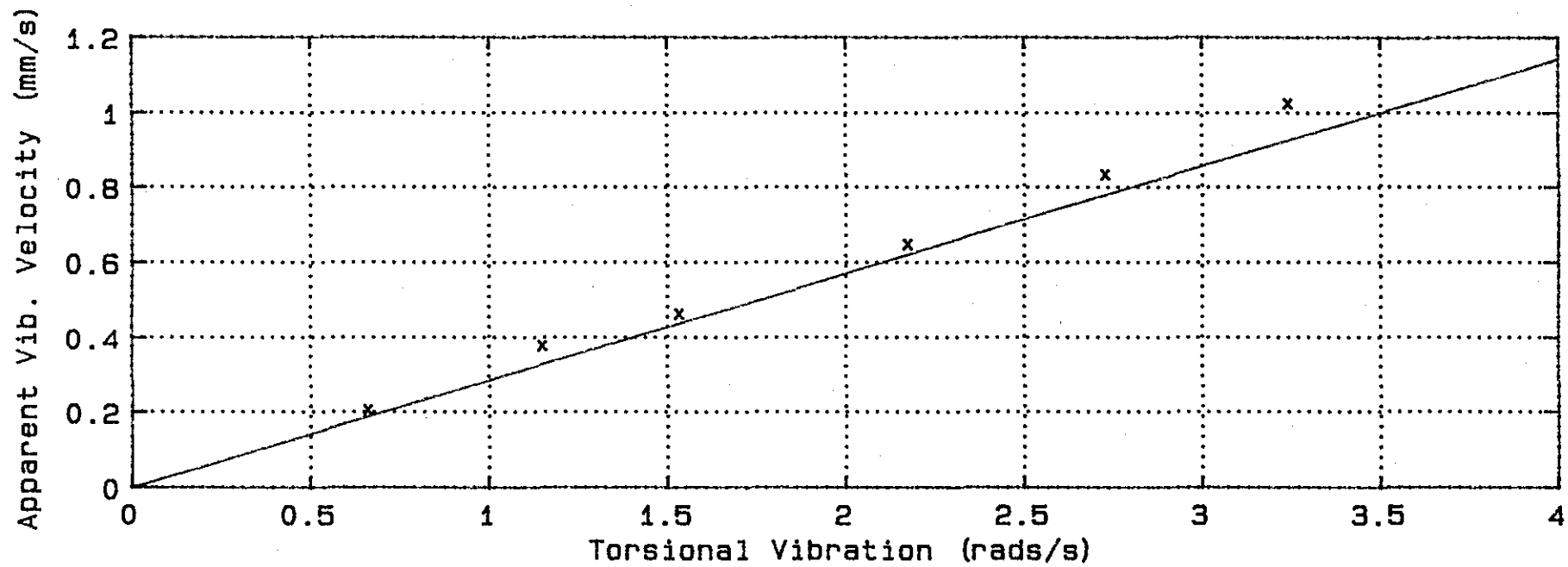
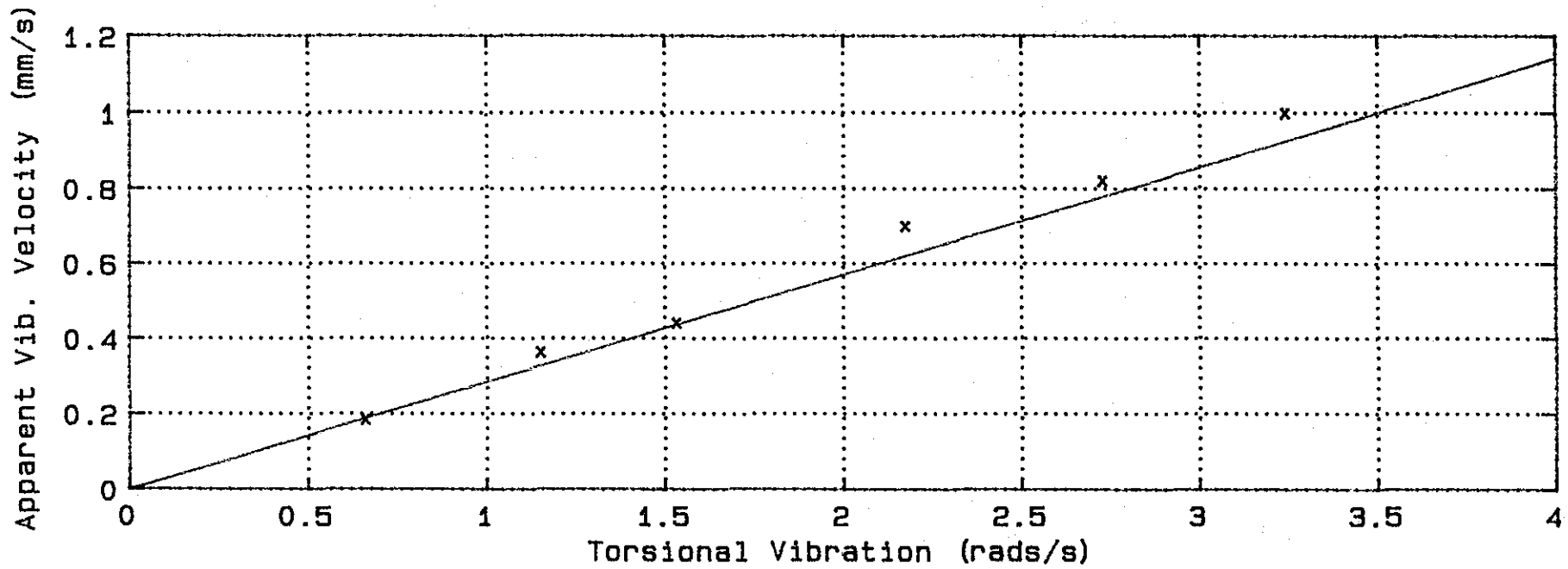


Figure 6: Effect of Torsional Vibration during In-Plane Vibration (a) Difference Frequency (b) Sum Frequency

FIG 6
(a)
(b)

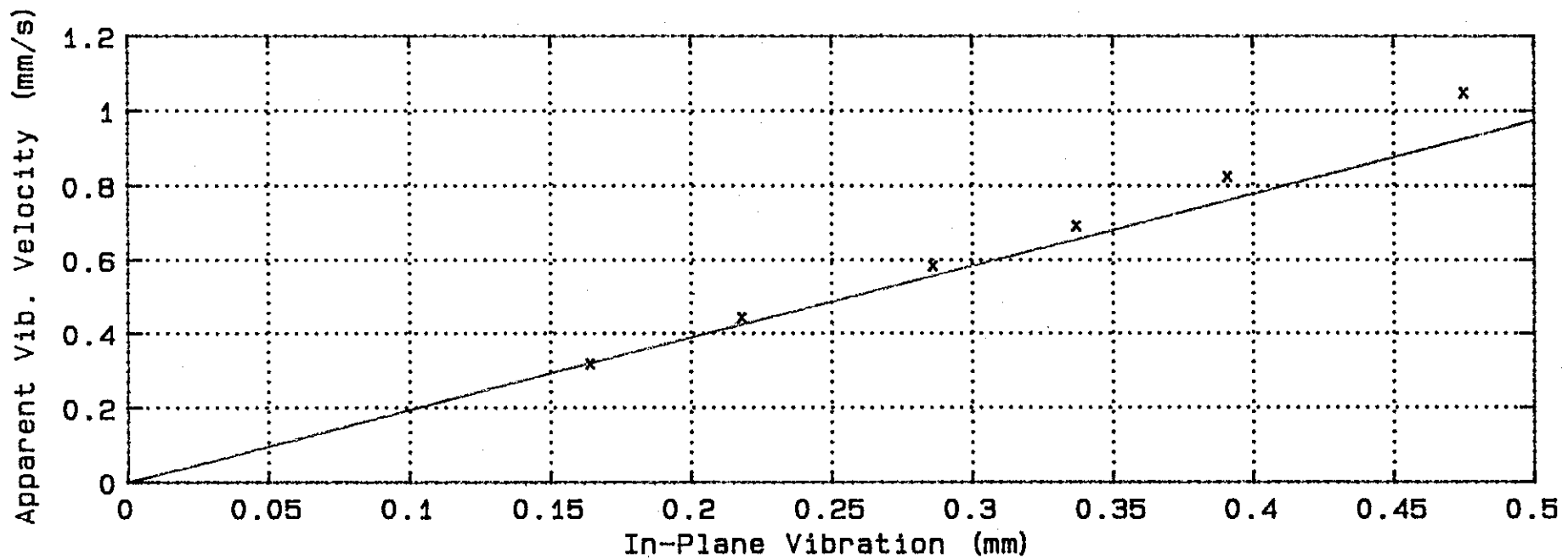
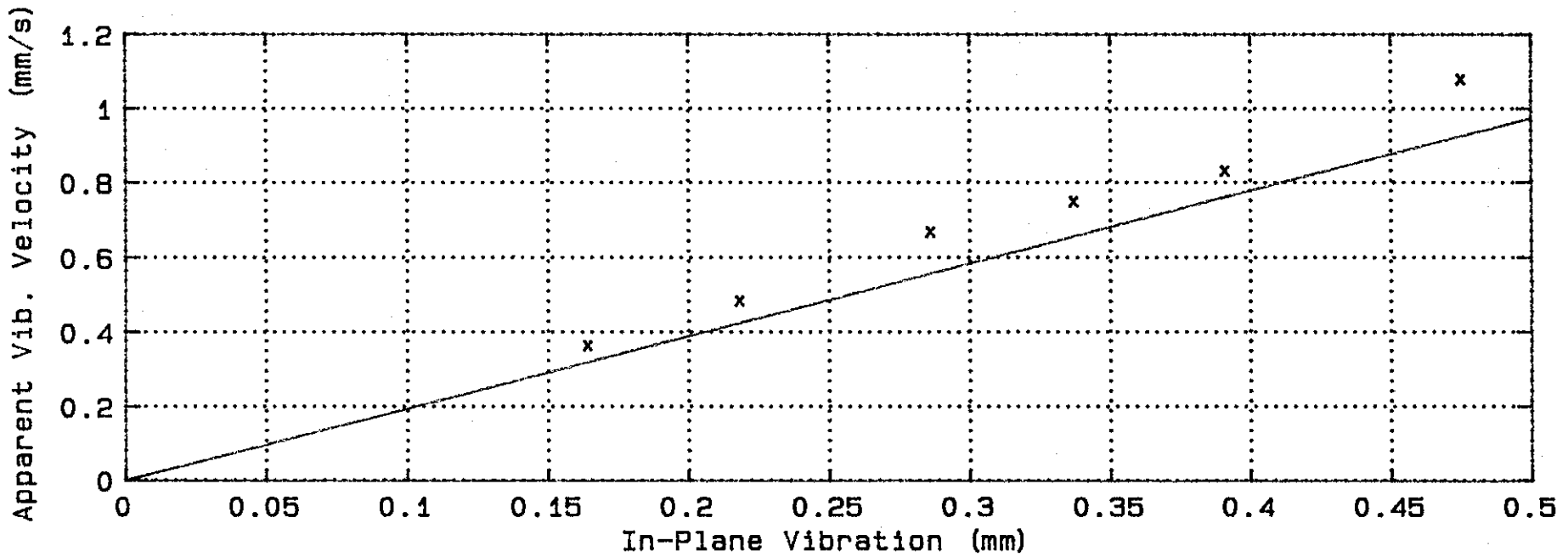


Figure 7: Effect of In-Plane Vibration during Torsional Vibration (a) Difference Frequency (b) Sum Frequency

FIG 7
(a)
(b)

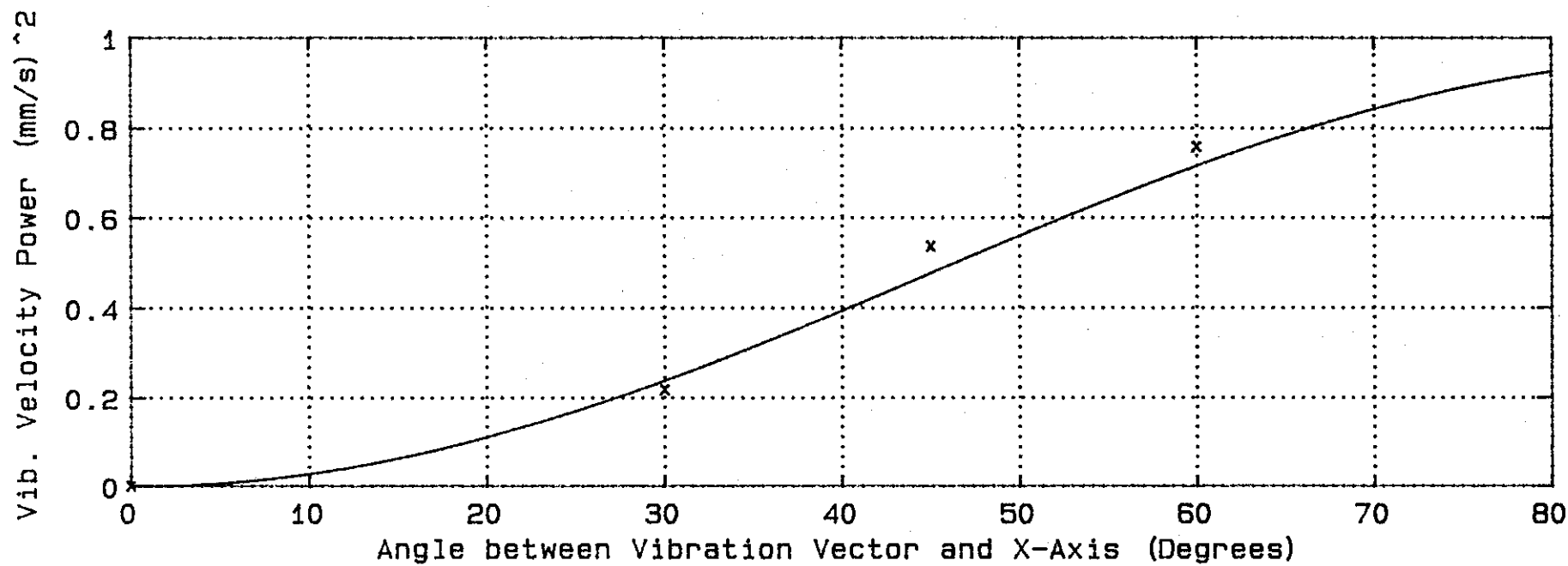
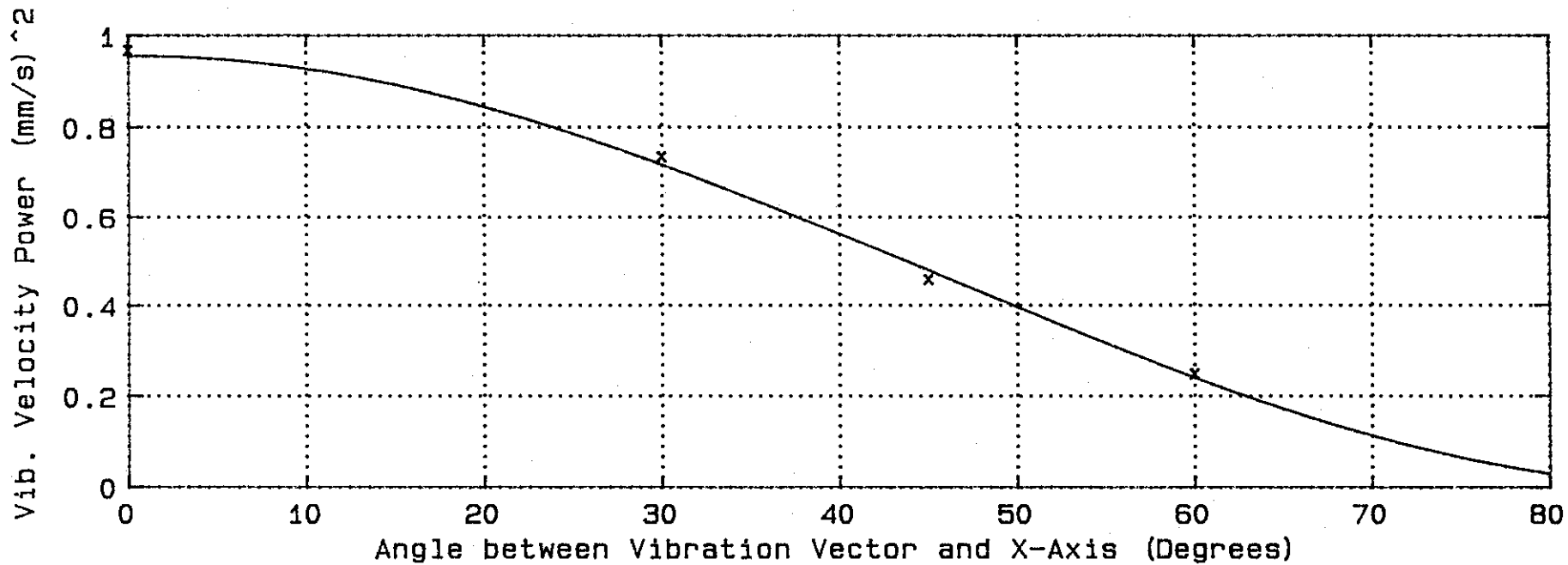


Figure 8: (a) Resolved X-Axis Component Fundamental Frequency (b) Resolved Y-Axis Component - Fundamental Frequency

FIG 8

(5)

(9)

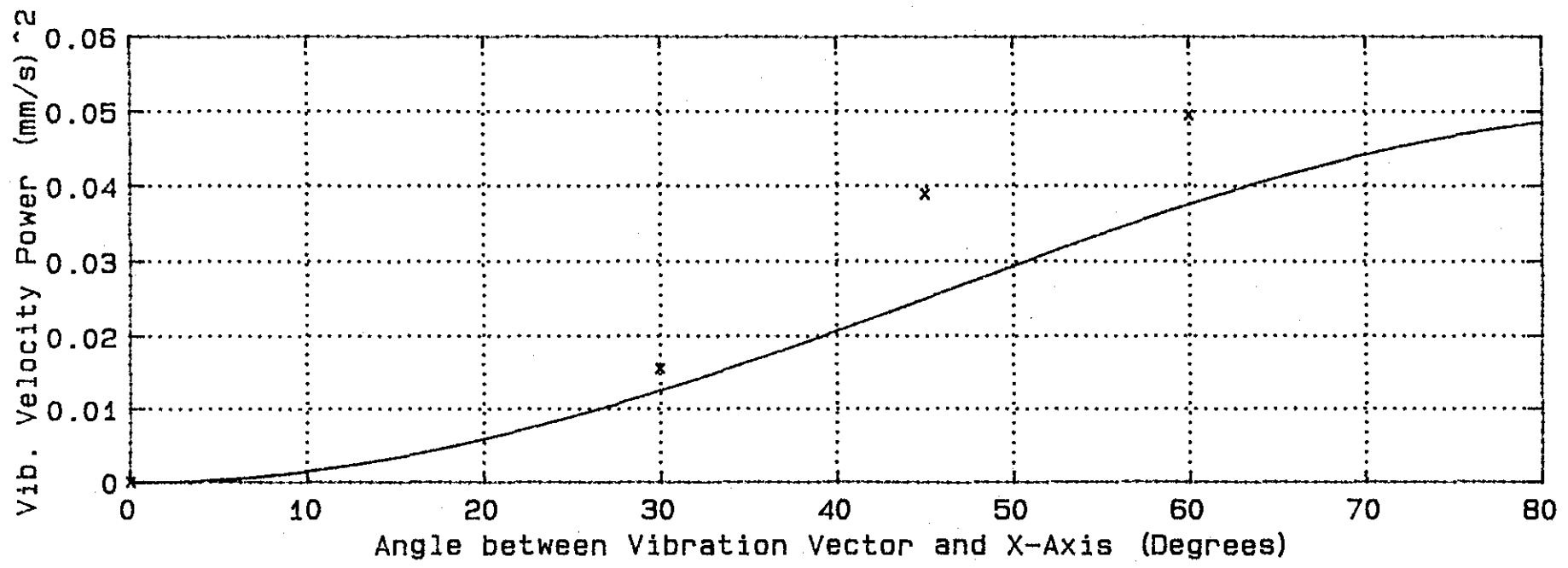
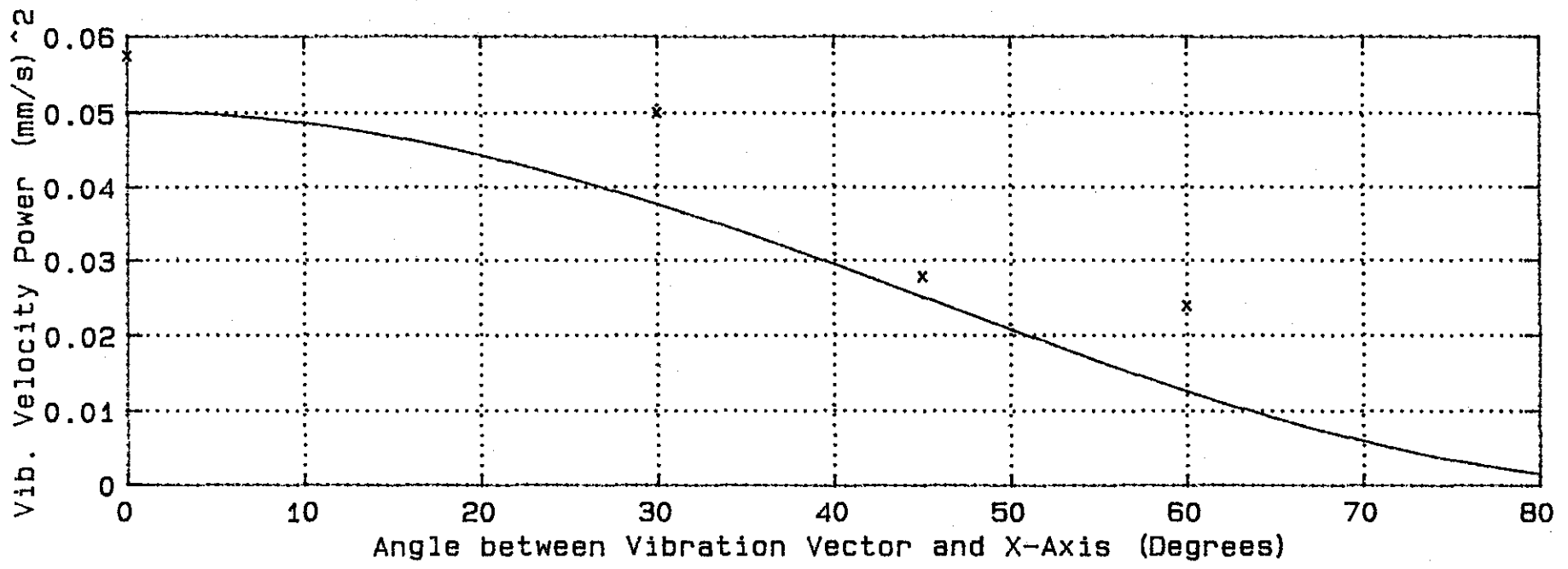


Figure 9: (a) Resolved X-Axis Component 2 x Fundamental Frequency (b) Resolved Y-Axis Component - 2 x Fundamental Frequency

FIG 9

(a)

(b)

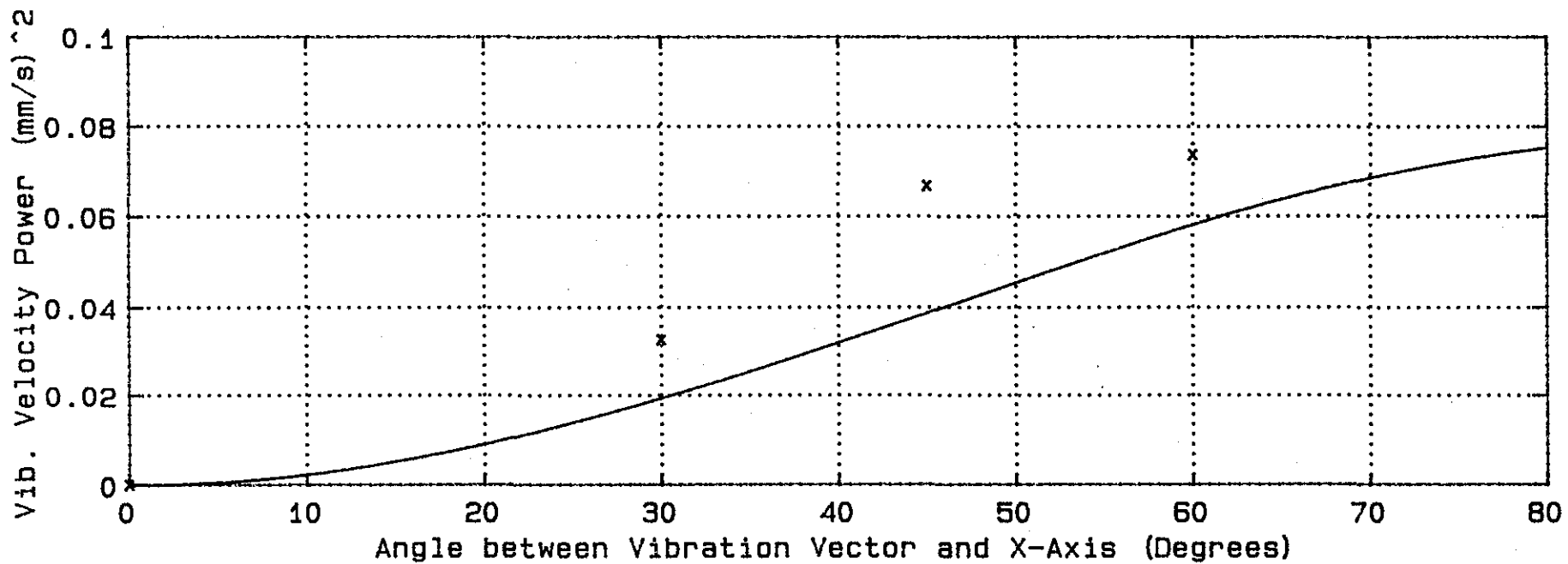
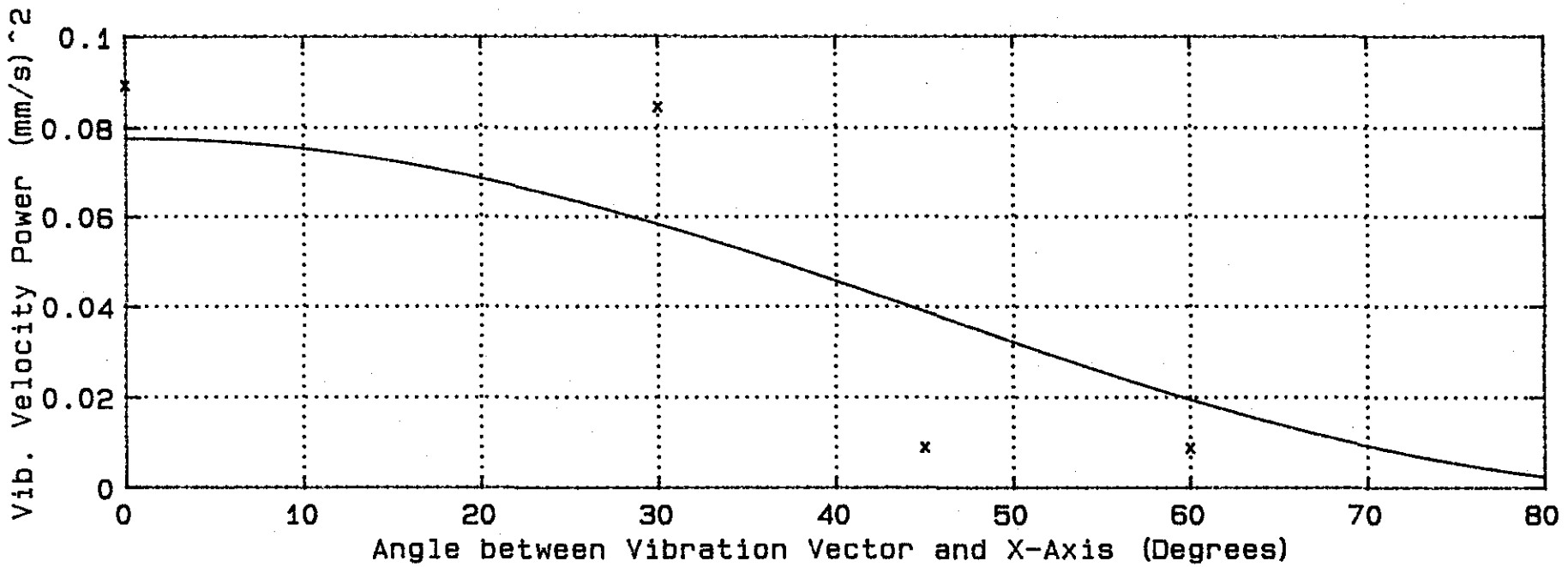


Figure 10: (a) Resolved X-Axis Component - 3 x Fundamental Frequency (b) Resolved Y-Axis Component - 3 x Fundamental Frequency

FIG 10

(a)

(b)